

Magnetotransport properties of spin-glass-like layered compounds $\text{La}_{1-x}\text{Sr}_{1+x}\text{CoO}_4$ ($0 \leq x \leq 0.40$)

M. Sánchez-Andújar^a, D. Rinaldi^b, R. Caciuffo^b, J. Mira^c, J. Rivas^c, M.A. Señarís-Rodríguez^{a,*}

^a *Dpto. Química Fundamental, Fac. Ciencias, Universidad de A Coruña, 15071 A Coruña, Spain*

^b *INFM and Dpto. di Fisica ed Ingegneria dei Materiali, Università Politecnica delle Marche-I-60131, Ancona, Italy*

^c *Dpto. Física Aplicada, Universidad de Santiago, 15782 Santiago de Compostela, Spain*

Received 11 November 2005; accepted 22 February 2006

Available online 3 May 2006

Abstract

We report the magnetic and transport properties of the cobalt layered mixed-oxides $\text{La}_{1-x}\text{Sr}_{1+x}\text{CoO}_4$ ($0 \leq x \leq 0.40$). An evolution towards an anomalous “cluster-glass”-like behavior as x increases has been found. The onset of the ferromagnetic order in the layered phases occurs at around 150 K followed by a blocking process around 125 K. Also, present in the magnetic response of these materials is the signal coming from small intergrowths of a perovskite phase, also detected by TEM, although invisible for powder-X-ray diffraction. From the electrical point of view these materials are semiconducting and their resistivity decreases upon doping. Most interestingly, at low temperature these layered compounds show rather large magnetoresistance (MR). The highest effect is found in the sample with $x = 0.20$ that shows a magnetoresistance $\text{MR}_{\text{max}} = -24\%$ at $T = 15$ K under a field $H_{\text{max}} = 50$ kOe.

© 2006 Elsevier SAS. All rights reserved.

Keywords: Layered-perovskites; Cobalt oxides; Magnetic and transport properties; Magnetoresistance

1. Introduction

The influence of dimensionality in the magnetism and electrical conductivity of perovskite and Ruddesden–Popper-type mixed oxides has been studied in the last few decades [1]. More recently a renewed interest in this topic has arisen in connection with colossal magnetoresistance (CMR) discovered in manganese oxides [2], as this property is affected by the effective dimensionality of the structure. For example, an increase in the 2D character of the structure in Ruddesden–Popper systems, that enhances electronic correlations, can lead to higher magnetoresistance, even at lower temperatures [3–6].

Apart from manganese oxides, magnetoresistance has been found in other systems such as cobalt mixed oxides with perovskite structure [7,8]. These cobalt compounds are another specially interesting family of compounds that have been the focus of numerous studies since the 1950s [9–11], in par-

ticular the lanthanum materials. In this context, LaCoO_3 has been found to exhibit remarkable transport and magnetic properties as a result of thermally induced transitions from low-spin (LS: $t^6 e^0$) to higher-spin states of the trivalent cobalt ions (intermediate spin IS: $t^5 e^1$, high spin HS: $t^4 e^2$) [10,12]. Those early studies also showed that whereas LaCoO_3 shows high resistivity and antiferromagnetic exchange interactions, the $\text{La}_{1-x}\text{Sr}_x\text{CoO}_3$ materials evolve towards a ferromagnetic metallic behavior as the doping degree increases [11]. The evolution takes place smoothly and a number of different magnetic and electrical behaviors are present for different degrees of doping and different temperature intervals [13–15]: superparamagnetism, spin-glass/cluster glass behavior and so forth, semi-conducting/metallic behaviors and even metal-insulator transitions as a function of temperature. Such complex electric and magnetic behaviors have been explained on the basis of an electronic phase segregation that gives rise to hole-rich ferromagnetic regions within a hole-poor matrix, that coexist within the same crystallographic phase [13].

More recently, this $\text{La}_{1-x}\text{Sr}_x\text{CoO}_3$ system has also attracted attention in connection with MR, that specially occur in the

* Corresponding author. Tel.: (+34) 981167000; fax: (+34) 981167065.
E-mail address: tonasr@udc.es (M.A. Señarís-Rodríguez).

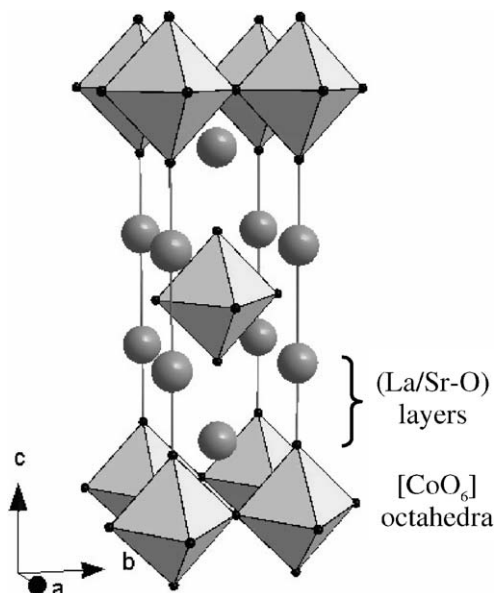


Fig. 1. Schematic representation of the K_2NiF_4 structure displayed by the $La_{1-x}Sr_{1+x}CoO_4$ compounds.

low-doped samples with $x < 0.20$ with a $MR_{\max}(x = 0.07) = -40\%$ at $T = 40$ K under $H = 60$ kOe [7].

Contrary to the case of the 3D Co-perovskites, the study of the magnetic and transport properties of other Co-Ruddlesden–Popper phases is a relatively much less explored area, although also very interesting as shown by the recent discovery of superconductivity in layered cobalt oxides [16].

In this work we focus in the properties of the $La_{1-x}Sr_{1+x}CoO_4$ compounds, which are the $n = 1$ members of the Ruddlesden–Popper series and exhibit the so-called K_2NiF_4 structure (Fig. 1). As it can be seen, this structure that is the two-dimensional analogue of the 3D perovskite consists of perovskite layers of corner-sharing $[CoO_6]$ octahedra that are separated from one another by the presence of rock-salt type (La/Sr–O) layers along the c -axis.

From the physical point of view, the $LaSrCoO_4$ compound is the relatively better characterized member of the series, even if there are discrepancies in the literature about its magnetic behavior and the spin configuration of the cobalt ions. In this context whereas Moritomo et al. [17] found a spin-glass behavior in $LaSrCoO_4$ single crystals, Demazeau et al. [18] described a paramagnetic behavior for this compound (after subtraction of the ferromagnetic contributions from ferromagnetic impurities) and other authors reported a ferromagnetic behavior [19]. Concerning the spin configuration of the trivalent cobalt ions, it has first been proposed that low spin (LS) and high spin (HS) Co^{3+} ions coexist in the material [18]. Nevertheless, more recent work gives evidence for an intermediate spin (IS) at the trivalent cobalt ions, which would be favored in this structure [17].

When $LaSrCoO_4$ is further doped with Sr^{2+} , and mixed valence $3+/4+$ is induced in the cobalt ions, the $La_{1-x}Sr_{1+x}CoO_4$ compounds evolve towards a ferromagnetic-like behavior and their resistivity decreases [20], although there are not detailed studies available in the literature about the evolution of those properties as a function of x .

In a previous work, using an appropriate synthetic method we were able to prepare Sr-doped $La_{1-x}Sr_{1+x}CoO_4$ ($0 \leq x \leq 0.40$) enlarging the compositional range of solid solution available so far [21]. Also, we carried out their structural and microstructural characterization of the obtained compounds [21].

According to the powder X-ray diffraction (PXRD) results of this study [21], these compounds with $0 \leq x \leq 0.40$ are single-phase crystalline materials, and the presence of perovskite-related phases (that often appear as impurities of the Ruddlesden–Popper phase with $n = 1$) is not detected.

On the other hand, TGA results showed that while the $x = 0$ compound is oxygen stoichiometric, as the Sr content gets higher ($x > 0$) a small but increasing oxygen-deficiency (δ) appears, so that $\delta_{\max}(x = 0.40) = 0.06$.

According to the corresponding Rietveld refinement of the PXRD data [21] these $La_{1-x}Sr_{1+x}CoO_4$ samples ($0 \leq x \leq 0.40$) crystallize in the tetragonal K_2NiF_4 structure, space group $I4/mmm$, in which the La^{3+} and Sr^{2+} ions are randomly distributed in 9-coordinated sites while the cobalt ions are in a tetragonally-elongated octahedral environment. Upon doping the distortion of the $[CoO_6]$ octahedral decreases, as the longer apical Co–O(1) distance decreases with x while the shorter equatorial Co–O(2) distance remains almost constant. The detailed evolution of cell parameters and bond lengths upon doping can be found in reference [21].

On the other hand, TEM studies revealed the presence, in some microcrystals, of stacking defects along the c -axis that were identified as perovskite slices of different widths, intergrown with the predominant K_2NiF_4 structure [21].

With this background and using the previously described samples, we have reexamined in detail the evolution of the magnetic and transport behavior of the $La_{1-x}Sr_{1+x}CoO_4$ system upon doping and explored the influence of dimensionality on these properties. The most outstanding results of this study are presented in this paper, where we also describe for the first time in these compounds the influence of the magnetic field on their electrical properties.

2. Experimental

The samples with nominal composition $La_{1-x}Sr_{1+x}CoO_4$ $x = 0, 0.10, 0.20, 0.30$ and 0.40 used for this study were prepared by the decomposition of the corresponding mixture of nitrates in the presence of KNO_3 , as reported in Ref. [21], where their structural and microstructural characterization is also described and discussed.

For the magnetic characterization of these materials we carried out both DC and AC measurements, as these later are specially useful to reveal magnetic transitions in complex systems.

In this context, the DC magnetic properties of these compounds were studied by means of a Quantum Design MPMS Squid magnetometer. Zero-field-cooled (ZFC) and field-cooled (FC) magnetic susceptibility data were obtained under a field of 1000 Oe in the temperature range $4 \leq T$ (K) ≤ 300 . Hysteresis loops in ZFC conditions were obtained at 5 K varying the field up to ± 50 kOe.

On the other hand, the linear and non-linear components of the AC magnetic susceptibility were measured as a function of temperature with a Lake Shore 7000 system using the mutual-inductance technique. Data were collected on warming from 15 to 300 K, after zero-field cooling of the sample. The calibration was performed with a $\text{Gd}_2(\text{SO}_4)_3 \cdot 8\text{H}_2\text{O}$ paramagnetic salt, having the same shape and size as the investigated samples.

The four-probe electrical resistivity of pressed pellets was measured as a function of temperature in the range $4 \leq T$ (K) ≤ 300 at zero magnetic field ($H = 0$) and using a constant field between $0 < H$ (kOe) < 50 in a homemade device. In this device the magnetoresistance of the samples was measured at a constant temperature using a field ranging between 0 and 50 kOe.

Seebeck coefficients were measured in the temperature interval $77 \leq T$ (K) ≤ 450 using a homemade device similar to the one described in Ref. [22].

3. Results

3.1. Magnetic properties

First of all we will refer to the magnetic properties of the as-prepared $x = 0$ compound LaSrCoO_4 for which, as already mentioned in the introduction, different magnetic behaviors have been previously described [17–20].

In our study, when measuring the magnetic susceptibility, $\chi_m(T)$, of the $x = 0$ sample we found a complex curve shape in both the DC and AC measurements (Fig. 2). As it can be seen in this figure, the susceptibility changes markedly below some critical temperatures, marked by arrows, and specially remarkable are the rises below ~ 220 and ~ 150 K.

The DC $\chi_m(T)$ data of this $x = 0$ sample follow a Curie–Weiss law for $\sim 250 < T$ (K) < 300 , and from the corresponding fitting we obtained an effective magnetic moment per cobalt ion $\mu_{\text{eff-Co}} = 2.80 \mu_B$ and a Weiss constant with a small negative value $\theta = -14$ K.

As the doping degree increases ($x > 0$), the DC magnetic susceptibility of the samples increases markedly with x below ~ 220 K (Fig. 3). On the other hand, a fit of the $\chi_m(T)$ data to a

Curie–Weiss law in the temperature range $220 < T$ (K) < 300 provides an indicator of how the effective mean atomic moment per cobalt ion, $\mu_{\text{eff-Co}}$ and the mean interatomic exchange interactions, as expressed by the Weiss constant, are evolving with x . As shown in Table 1, such curve fitting gives a $\mu_{\text{eff-Co}}$ that changes very little with x , and a Weiss constant that increases from a small negative value for $x = 0$ to a rather high positive value for $x = 0.40$.

The temperature dependence of the real part of the AC susceptibility, χ' , of these samples with $x > 0$ is shown in Fig. 4. As it can be seen, the sharp rise of the susceptibility below ~ 220 K is followed by a shoulder at ~ 150 K and a maximum at ~ 125 K. It is also remarkable that as x increases the intensity of these last two features increases markedly and their position slightly shifts towards higher temperatures.

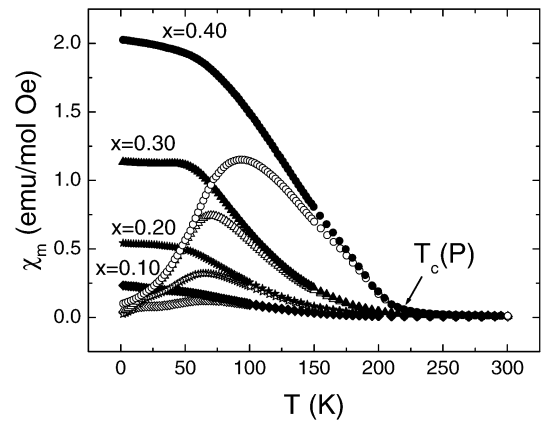


Fig. 3. DC ZFC (open symbols) and FC (closed symbols) molar magnetic susceptibility of $\text{La}_{1-x}\text{Sr}_{1+x}\text{CoO}_4$ ($0.10 \leq x \leq 0.40$) measured under a field $H = 1000$ Oe.

Table 1

Effective magnetic moment of the Co ions $\mu_{\text{eff-Co}}$ and Weiss constant (θ) of $\text{La}_{1-x}\text{Sr}_{1+x}\text{CoO}_4$ ($0 \leq x \leq 0.40$)

	$x = 0$	$x = 0.10$	$x = 0.20$	$x = 0.30$	$x = 0.40$
$\mu_{\text{eff-Co}}$ (μ_B)	2.80	2.72	2.93	2.90	2.91
θ (K)	-14	92	133	168	200

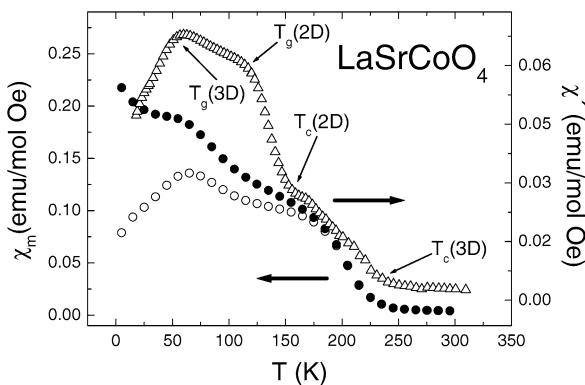


Fig. 2. DC [ZFC (opened circle) and FC (closed circle)] and AC (opened triangle) molar magnetic susceptibility data for LaSrCoO_4 ($x = 0$). The DC results were obtained under $H = 1000$ Oe and the AC data were taken with a driving field amplitude $H_0 = 2.5$ Oe, oscillating at a frequency of 1 kHz.

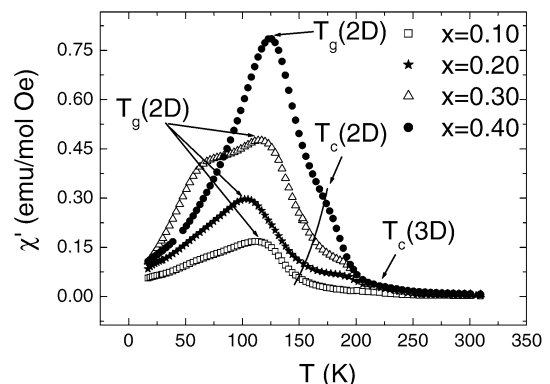


Fig. 4. AC magnetic susceptibility of $\text{La}_{1-x}\text{Sr}_{1+x}\text{CoO}_4$ $0.10 \leq x \leq 0.40$ compounds measured with a driving field amplitude $H_0 = 2.5$ Oe, oscillating at a frequency of 1 kHz.

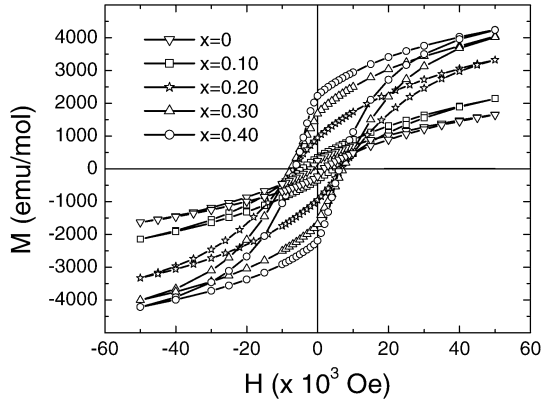


Fig. 5. ZFC magnetization versus applied field H of $\text{La}_{1-x}\text{Sr}_{1+x}\text{CoO}_4$ ($0 \leq x \leq 0.40$) measured at $T = 5$ K.

On the other hand, the $M(H)$ curves at $T = 5$ K of these samples ($0 \leq x \leq 0.40$) are shown in Fig. 5. Specially interesting is the fact that magnetization increases with x and also the lack of saturation of these curves under the highest field used (50 kOe).

3.2. Transport properties

The $\text{La}_{1-x}\text{Sr}_{1+x}\text{CoO}_4$ ($0 \leq x \leq 0.40$) materials are all semi-conducting with a rather high resistivity, ρ , even if it decreases as the doping degree increases (Fig. 6).

In the temperature range $250 < T$ (K) < 300 , the resistivity data of all the samples can be fitted to the non-adiabatic small polarons expression [23]:

$$\rho \propto T^{3/2} \exp[E_a/k_B T]. \quad (1)$$

Meanwhile, for $80 < T$ (K) < 220 the temperature dependence of the resistivity is better fitted to the Mott Variable-Range Hopping (VHR) expression [23]:

$$\rho \propto \exp[T_0/T]^{1/(d+1)} \quad (2)$$

where d is the dimensionality of the system and T_0 is related to the density of states at the Fermi energy and the localization length.

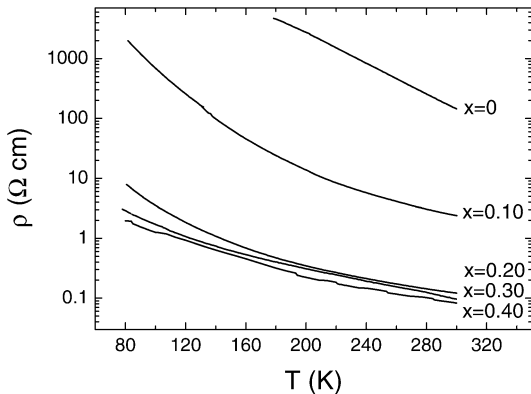


Fig. 6. Electrical resistivity versus temperature of $\text{La}_{1-x}\text{Sr}_{1+x}\text{CoO}_4$ ($0 \leq x \leq 0.40$) for $80 \leq T$ (K) ≤ 300 .

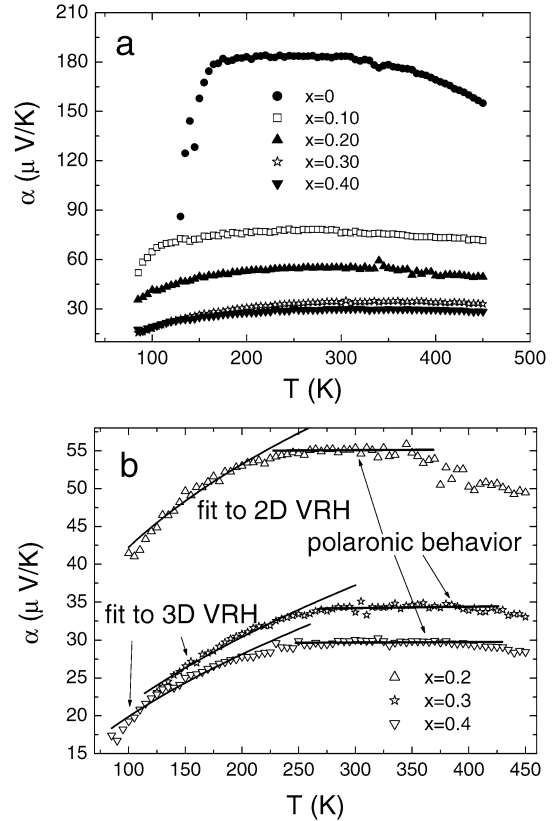


Fig. 7. (a) Temperature dependence of the Seebeck coefficient of $\text{La}_{1-x}\text{Sr}_{1+x}\text{CoO}_4$ ($0 \leq x \leq 0.40$) in the temperature range $100 \leq T$ (K) ≤ 450 . (b) Fitting of the Seebeck data from the samples with $x = 0.20, 0.30$ and 0.40 to 2D and 3D VRH and to polaronic behavior in different temperatures intervals.

For $x \leq 0.20$ the data are most consistent with Eq. (2) considering $d = 2$ (2D behavior) while for $x \geq 0.30$ the best fit is obtained for $d = 3$ (3D behavior).

Measurements of thermoelectric power versus temperature, $\alpha(T)$, are shown in Fig. 7 for these samples $0 \leq x \leq 0.40$. As it can be seen the Seebeck coefficient (α) is in all cases positive, indicating that the charge carriers are holes; and as x increases its value decreases, indicating that the number of charge carriers is increasing. It is interesting to note that in the case of the $x = 0$ sample, where all the cobalt ions are expected to have a formal valence of 3+, the Seebeck coefficient is much lower than expected, as compared with the very high values found in the corresponding 3D perovskite LaCoO_3 [12].

As for the temperature dependence of the Seebeck coefficient of these samples, the plateau that appears for $T > 250$ K is a signature of a small-polaron transport regime [23]. Meanwhile, for $T < 250$ K the Seebeck coefficient data can be fitted to the following expression [24]:

$$\alpha = AT^{1/(n+1)} \quad (3)$$

that corresponds to a variable range hopping mechanism, with $n = 2$ (2D behavior) for $x \leq 0.20$ and with $n = 1$ (3D behavior) for $x > 0.20$, see Fig. 7(b).

To study the influence of the magnetic field on the electrical resistivity of these materials, we measured $\rho(T)$ under a constant field of 40 kOe. As can be seen in a typical example

in Fig. 8, at low temperatures the magnetic field reduces the samples' resistivity, and the effect becomes more pronounced as the temperature decreases. For this reason, we measured the magnetoresistance of these samples at the lowest possible temperature, with the limitation imposed by the high resistivity of these samples at low temperatures. For example, in the low-doped sample $x = 0.1$, MR could only be measured above 55 K. The obtained MR values [MR defined as $(\rho(H) - \rho(0))/\rho(0)$] are shown graphically in Figs. 9(a) and (b). As it can be seen, the highest values of MR are obtained for $x = 0.20$ for which $MR_{\max} = -25\%$ at $T = 15$ K and $MR = -14\%$ at $T = 25$ K under an $H_{\max} = 50$ kOe.

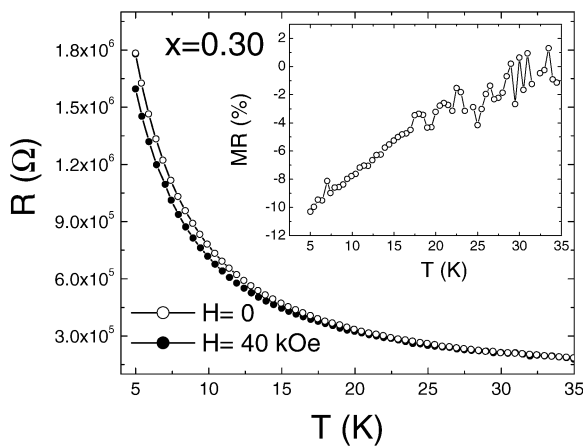


Fig. 8. Temperature dependence of the electrical resistance of the $x = 0.30$ sample in the absence of a magnetic field and under a field of 40 kOe ($5 \leq T$ (K) ≤ 35). Inset: MR versus temperature under a field of 40 kOe in this same interval.

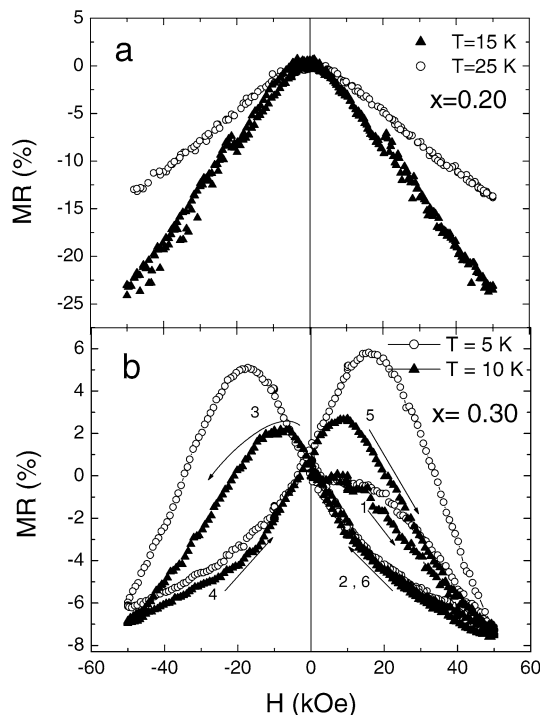


Fig. 9. Field dependence of the electrical resistivity of the $La_{1-x}Sr_{1+x}CoO_4$ samples: (a) $x = 0.20$, measured at 15 and 25 K. (b) $x = 0.30$, measured at 5 and 10 K.

4. Discussion

The magnetic and transport properties of the $La_{1-x}Sr_{1+x}CoO_4$ compounds are rather complex.

Starting by the sample with nominal composition $LaSrCoO_4$ ($x = 0$), that in principle should be a Co^{3+} compound, its magnetic and electrical behaviors are rather surprising.

In this context, in view of the obtained magnetic results one would think that $LaSrCoO_4$ shows a spin-glass-like behavior, as other authors have already noted [17]. But one has to be very careful with the obtained results and their interpretation as some features, of both the DC and AC susceptibility curves, show clear analogies with those typical for low-doped $La_{1-x}Sr_xCoO_3$ perovskite [15,25]. In fact, comparison with previous results leads us to identify the features marked in Fig. 2 as T_c (3D) at $T \sim 250$ K and T_g (3D) at $T \sim 60$ K with the Curie temperature and glass-freezing temperature of the minority low-doped $La_{1-x}Sr_xCoO_3$ perovskite phases [15].

We therefore assume that the sample with $x = 0$ and nominal composition $LaSrCoO_4$ is a mixture of a majority layered phases $La_{1-x}Sr_{1+x}CoO_4$ with $x > 0$ (and therefore 3+ and 4+ mixed-valence in the cobalt ions) and a minority phase $La_{1-x}Sr_xCoO_3$. This assumption is also supported by the fact that even if that impurity is not detected by means of powder X-ray diffraction, transmission electron microscopy reveals the presence of small intergrowths of a perovskite phase [21].

The results of the thermoelectric power of this sample of nominal composition $x = 0$ corroborate this picture: as already pointed out the Seebeck coefficient of this material is much lower than expected for a purely trivalent Co compound, result that reveals that the starting layered compound is in fact already doped with a certain number of holes, so that the compound nominal composition and the real composition are different.

Now, focusing in the magnetic signals coming from the layered phase we assign the shoulder seen in the AC curves around ~ 150 K to the ferromagnetic coupling in the 2D compound [T_c (2D)], while we attribute the maximum at ~ 125 K to a blocking process [T_B (2D)]. This features become more evident as x increases and as the samples evolve towards a “cluster-glass” behavior.

The evolution of the Weiss constant with x corroborates the increase in the strength of the ferromagnetic interactions as x gets higher.

On the other hand, the estimated effective magnetic moment per cobalt ion (Table 1) suggest an intermediate spin state configuration of the Co^{3+} ions in these bidimensional compounds ($IS: t^5 e^1$). Such configuration could be stabilized by the axially-elongated octahedral environment of the Co ions [17], revealed by the X-ray diffraction data. This feature has also been observed in other transition metal oxides such as in Sr–Ru–O system, where the dimensionality of structure influences the spin configuration of the transition metal ions [26].

From the electrical point of view, even if the resistivity of these materials decreases upon doping, the metallic behavior is not achieved even in the highest-doped sample at difference with the corresponding 3D compounds. Another remarkable result is the crossover behavior observed as a function of x for

$T < 250$ K: while both the resistivity and Seebeck data show a 2D VRH behavior in the $x \leq 0.20$ compounds they both do show a 3D VRH behavior in the $x > 0.20$ samples. This crossover between 2D and 3D VRH has been described in the literature for different compounds, for example high T_c superconducting materials [27,28]; or Ge–As alloys [29] in which a strong magnetic field can also provoke this crossover. It should be pointed out that this crossover is only electronic and does not affect the dimensionality of the crystal structure.

If we now analyse globally the results for these Sr-doped layered compounds and how they evolve with x , and compare them with the 3D analogues $\text{La}_{1-x}\text{Sr}_x\text{CoO}_3$ [13], we find clear analogies between the magnetic and transport properties of the two.

As mentioned before, in that extensively studied $\text{La}_{1-x}\text{Sr}_x\text{CoO}_3$ system it has been proposed [13] that upon doping the material segregates into two distinguishable electronic states that coexist within the same crystallographic matrix: hole-rich, metallic ferromagnetic regions where the cobalt ions are in the intermediate-spin configuration, and a hole-poor matrix similar to LaCoO_3 which experiences a thermally induced low spin to high spin transition. According to that model [13], corroborated in later investigations [15,25], for low Sr^{2+} -doping, the hole-rich regions are isolated from one another, show superparamagnetic behavior below a $T_c \approx 240$ K that changes very little with x , and the samples show semiconducting behavior. Long-range magnetic order via frustrated intercluster interactions occurs below a superparamagnetic freezing temperature T_B that increases with x . A magnetic percolation threshold is reached at $x_m \sim 0.20$, and for $x_m < x \leq 0.50$, the ferromagnetic hole-rich regions couple ferromagnetically to give bulk ferromagnetism below T_c . However, the electrical conduction in the ferromagnetic regions is modulated by the matrix, which has a spin state that varies with temperature, and that gives rise to a reentrant semiconducting behavior for $0.20 \leq x \leq 0.30$. Metallic behavior is found once the electrical percolation threshold x_c , ($x_c \sim 0.30$) is achieved, but the presence of the hole-poor matrix interpenetrating the metallic ferromagnetic regions persists and gives rise to peculiar magnetic behavior.

In view of the similarities we propose that in general the above model can also be extended to $\text{La}_{1-x}\text{Sr}_{1+x}\text{CoO}_4$ materials ($0 \leq x \leq 0.40$), taking into account the role played by the different dimensionality of the two crystal structures.

Of course, to do so, one has to take into account that the lower dimensionality of the crystal structure will influence and introduce differences in the spin state of the Co ions, the characteristics of the hole-poor and hole-rich regions as well as the magnetic and electrical connection between them. In this context the axially-elongated octahedral environment of the cobalt ions in the 2D K_2NiF_4 structure stabilizes an intermediate spin configuration in Co^{3+} ions, in the whole temperature interval studied, as difference with the thermal activated spin transition that occurs in the case of the 3D compounds.

On the other hand, it should be remember that the structure of both these K_2NiF_4 -phases and the perovskite compounds, that is based on corner-shared $[\text{CoO}_6]$ octahedra, that in the case of the 2D phase are just linked to other four $[\text{CoO}_6]$ octahedral

within the a – b plane, while they are linked to six in the three space directions in the case of the 3D perovskites.

As a consequence and as the Curie temperature depends on the number of nearest neighbors [30]:

$$T_c \approx 2zS(S+1)J/3k_B \quad (4)$$

where z = number of nearest neighbors, S = total spin angular momentum, J = exchange integral and k_B = Boltzmann constant).

T_c turns to be lower (and the ferromagnetic interactions weaker) in the layered compounds as compared to the corresponding 3D perovskites: T_c (2D) ~ 150 K vs T_c (3D) ~ 240 K.

In addition, the bandwidth $w \approx 2zb$ [31], that also depends on the number of neighbours z will be narrower in the case of the 2D compounds and will hinder stabilization of ferromagnetic interactions via double-exchange.

As a result, the 2D compounds show lower T_c , lower magnetization and lower conductivity than the corresponding 3D compounds.

These factors also explain why, contrary to the case of 3D samples, magnetic percolation has not been reached in these layered compounds that still show a cluster-glass-like behavior; and why they are also below the electrical percolation threshold and still show semiconducting properties.

The magnetoresistive effects of these 2D compounds can also be explained invoking this electronic phase segregation scenario. These samples display magnetoresistance effects at low temperatures, $T < 40$ K, where the ZFC and FC curves show a large split and where the samples exhibit a spin-glass or cluster-glass type of behavior by blocking of the ferromagnetic clusters. At low temperatures and at zero field the FM clusters are randomly aligned but, as the magnetic field increases the FM clusters tend to increase their size and align themselves with the field to minimize magnetic energy. In this situation the hopping probability of the charge carriers increases, the scattering of the electrons at the boundaries between the ferromagnetic regions gets reduced and negative magnetoresistance is observed.

In this context, similar MR effects have been found in other spin-glass materials, for example ($\text{La}_{1-x}\text{Sr}_x\text{CoO}_3$ ($x < 0.20$) [32], $\text{Gd}_{1-x}\text{Sr}_x\text{CoO}_3$ ($x \leq 0.30$) [8], $\text{Sr}_3\text{Fe}_{1.5}\text{Co}_{0.5}\text{O}_{6.67}$ [33], $\text{SrRu}_{1-x}\text{Fe}_x\text{O}_3$ [34], where the observed MR (high at low temperatures) is due to their glassy magnetic behavior. Recently, to explain the origin of the MR in the $\text{La}_{1-x}\text{Sr}_x\text{CoO}_3$ ($x < 0.2$) [35] it was argued that these systems are natural analogues of artificial structures consisting of nanoscale ferromagnetic particles embedded in a metallic or insulating matrix. $\text{La}_{1-x}\text{Sr}_{1+x}\text{CoO}_4$ compounds can be classified into this new kind of MR materials.

In addition for the doping level $x = 0.20$, that shows the highest magnetoresistance effect, there is another factor that can be contributing to the observed behavior: the compound with this composition is close to a crossover between 2D and 3D VRH. In this situation the magnetic field could be affecting the dimensionality of the sample's conductivity and changing it

from 2D to 3D. This in turn would lead to a more pronounced decrease of the resistivity and to the highest MR.

Finally, and although the MR effects found in these layered compounds are smaller than in the case of the corresponding 3D perovskites [32], it is worth noting that these values are relatively very high for a 2D phase. Note, for example, that the $n = 1$ $\text{La}_{1-x}\text{Sr}_{1+x}\text{MnO}_4$ layered manganites do not show any MR [36].

5. Conclusions

We have studied the magnetic and transport properties of the $\text{La}_{1-x}\text{Sr}_{1+x}\text{CoO}_4$ ($0 \leq x \leq 0.40$) bidimensional compounds and compared them with the corresponding 3D perovskites.

From the magnetic point of view, these materials evolve towards an anomalous “cluster-glass”-like behavior as x increases. The onset of the ferromagnetic order in the layered phases is seen to occur at around 150 K, followed by a blocking process around 125 K. The layered nature of these compounds prevents the percolation of the FM clusters, contrary to what happens in the 3D $\text{La}_{1-x}\text{Sr}_x\text{CoO}_3$ perovskites.

Other feature of the dimensionality is that in the layered compounds the spin configuration for the Co^{3+} that seems to be stabilized is the IS configuration ($t^5 e^1$).

Contrary to the case of the corresponding 3D perovskites, the layered structure maintains a semiconducting behavior in the whole compositional interval $0 \leq x \leq 0.40$, preventing electrical percolation to be achieved, even if the resistivity of the samples decreases as x increases.

A peculiarity of the electrical behavior of the layered $\text{La}_{1-x}\text{Sr}_{1+x}\text{CoO}_4$ compounds is that they show a crossover behavior between 2D VRH (for $x \leq 0.2$) and 3D VRH (for $x \geq 0.3$ for $T < 250$ K).

At low temperature these layered phases show rather large MR: $\text{MR}_{\text{max}}(x = 0.2) = -24\%$ at $T = 15$ K under a field of 50 kOe.

As in the case of the 3D perovskites, we explain the magneto-transport properties of these layered Co-compounds on the basis of an electronic phase segregation scenario.

Acknowledgements

We wish to thank the financial support from DGICYT, Ministerio de Ciencia y Tecnología (Spain) and EU (FEDER) under project MAT 2004-05130-C02. We are also indebted to Prof. J.B. Goodenough (Texas Materials Institute–University of Texas at Austin, USA) for fruitful discussions.

References

- [1] R.A. Mohan Ram, L. Ganapathi, P. Ganguly, C.N.R. Rao, J. Solid State Chem. 63 (1986) 138.

- [2] R. Von Helmolt, J. Wecker, B. Holzapfel, L. Schultz, K. Samwer, Phys. Rev. Lett. 71 (1993) 2331.
- [3] R. Mahesh, R. Mahendiran, A.K. Raychaudhuri, C.N.R. Rao, J. Solid State Chem. 122 (1996) 448.
- [4] Y. Moritomo, A. Asamitsu, H. Kuwahara, Y. Tokura, Nature 380 (1996) 141.
- [5] T. Kimura, Y. Tokura, Annu. Rev. Mater. Sci. 30 (2000) 451.
- [6] S. Ghosh, P. Adler, Solid State Commun. 116 (2000) 585.
- [7] R. Mahendiran, A.K. Raychaudhuri, Phys. Rev. B 54 (1996) 16044.
- [8] C. Rey Cabezedo, M. Sánchez Andújar, J. Mira, A. Fondado, J. Rivas, M.A. Señaris Rodríguez, Chem. Mater. 14 (2002) 493.
- [9] J.B. Goodenough, J. Phys. Chem. Solids 6 (1958) 287.
- [10] P.M. Raccach, J.B. Goodenough, Phys. Rev. 155 (1967) 932.
- [11] P.M. Raccach, J.B. Goodenough, J. Appl. Phys. 39 (1968) 1209.
- [12] M.A. Señaris-Rodríguez, J.B. Goodenough, J. Solid State Chem. 116 (1995) 224.
- [13] M.A. Señaris-Rodríguez, J.B. Goodenough, J. Solid State Chem. 118 (1995) 323.
- [14] M. Itoh, I. Natori, S. Kubota, K. Motoya, J. Phys. Soc. Jpn. 63 (1994) 1486.
- [15] R. Caciuffo, D. Rinaldi, G. Barucca, J. Mira, J. Rivas, M.A. Señaris Rodríguez, P.G. Radaelli, D. Fiorani, J.B. Goodenough, Phys. Rev. B 59 (1999) 1068.
- [16] K. Takada, H. Sakurai, E. Takayama-Muromachi, F. Izumi, R.A. Dilanian, T. Sasaki, Nature 422 (2003) 53.
- [17] Y. Moritomo, K. Higashi, K. Matsuda, A. Nakamura, Phys. Rev. B 55 (1997) 14725.
- [18] G. Demazeau, Ph. Courbin, G. Le Flem, M. Pouchard, P. Hagenmuller, J.L. Soubeyrou, I.G. Main, G.A. Robins, Nouveau J. Chim. 3 (1979) 171.
- [19] Y. Furukawa, S. Wada, Y. Yamaha, J. Phys. Soc. Jpn. 62 (1993) 1127.
- [20] C.N.R. Rao, P. Ganguly, K.K. Singh, R.A. Mohan Ram, J. Solid State Chem. 72 (1988) 14.
- [21] M. Sánchez Andújar, M.A. Señaris Rodríguez, Solid State Sci. 6 (2004) 21.
- [22] J.B. Goodenough, J.S. Zhou, J. Chan, Phys. Rev. B 50 (1994) 3025.
- [23] N. Mott, Conduction in Non-Crystalline Materials, Clarendon Press, Oxford, 1993.
- [24] B. Fisher, J. Genosar, L. Patlagan, G.M. Reisner, C.K. Subramaniam, A.B. Kaiser, Phys. Rev. B 50 (1994) 4118.
- [25] G. Baio, G. Barucca, R. Caciuffo, D. Rinaldi, J. Mira, J. Rivas, M.A. Señaris Rodríguez, D. Fiorani, J. Phys.: Condens. Matter 12 (2000) 1.
- [26] M. Itoh, M. Shikano, T. Shimura, Phys. Rev. B 51 (1995) 16432.
- [27] B. Ellman, H.M. Jaeger, D.P. Katz, T.F. Rosenbaum, A.S. Cooper, G.P. Espinosa, Phys. Rev. B 39 (1989) 9012.
- [28] P. Mandal, A. Poddar, B. Ghosh, P. Choudhury, Phys. Rev. B 43 (1991) 13102.
- [29] I. Shlimak, M. Kaveh, M. Yosefin, M. Lea, P. Fozooni, Phys. Rev. Lett. 68 (1992) 3076.
- [30] C. Kittel, Introduction to Solid State Physics, John Wiley & Sons, New York, 1986.
- [31] J.B. Goodenough, Magnetism and the Chemical Bond, John Wiley & Sons, New York, 1963.
- [32] R. Mahendiran, A.K. Raychaudhuri, A. Chainani, D.D. Sarma, J. Phys.: Condens. Matter 7 (1995) 561.
- [33] M. Sánchez-Andújar, J. Mira, J. Rivas, M.A. Señaris-Rodríguez, J. Mag. Mater. 272–276 (2004) 855.
- [34] A. Mamchik, I.W. Chen, Appl. Phys. Lett. 82 (2003) 613.
- [35] J. Wu, J.W. Lynn, C.J. Glinka, J. Burley, H. Zheng, J.F. Mitchell, C. Leighton, Phys. Rev. Lett. 94 (2005) 37201.
- [36] Y. Moritomo, Y. Tomioka, A. Asamitsu, Y. Tokura, Phys. Rev. B 51 (1995) 3297.